On the Energy Flow in Piezoelectric Energy Harvesting with SSHI Interface

Junrui Liang and Wei-Hsin Liao[*]

Smart Materials and Structures Laboratory, Department of Mechanical and Automation Engineering,
The Chinese University of Hong Kong, Shatin, N. T., Hong Kong, China

ABSTRACT

In previous researches on piezoelectric energy harvesting, the foci were mostly on the amount of energy that can be harvested from the vibrating structures. The harvesting efficiency can be greatly improved with synchronized switch harvesting on inductor (SSHI). However, another portion of energy may be dissipated in the conditioning circuits of the treatment. In this paper, it is aimed to study on the functional relationship between the harvested energy and dissipated energy in the piezoelectric energy harvesting with SSHI interface. In addition, both energy harvesting and dissipation extract energy from the vibrating structure, and consequently bring out structural damping. Combining these two energy flows, the total effect of SSHI on structural damping is also discussed. Three experiments are performed, with the same piezoelectric cantilever based SSHI device, in order to measure the performances of energy harvesting, energy dissipation, and structural damping. The experimental results show good agreement with theoretical analyses.

Keywords: piezoelectric, SSHI, energy harvesting, energy dissipation, structural damping

1. INTRODUCTION

Different from the traditional sensor systems, the power supply for the wireless sensor networks (WSNs) is an issue. Yet, nowadays, most of the devices used in WSNs are still powered by batteries. The use of batteries in these devices restricts both their lifetime and installation in places where batteries are hard to be replaced. Such a problem could be hopefully overcome with the development on the techniques of *energy harvesting* (also known as *power harvesting* and *energy scavenging*). With these techniques, ambient energy in certain forms can be converted, stored in electrical form, and so as to power the wireless electronics. For example, with its electromechanical coupling characteristic, the piezoelectric material can be utilized to scavenge the mechanical energy associated with ambient vibration.

Most of the recent researches on piezoelectric energy harvesting (PEH) have focused on improving the efficiency of PEH devices with respect to three main considerations, i.e. piezoelectric configuration, circuitry and energy storage [1]. With the introduction of switching components, the circuitry design shows a good potential to provide flexible and effective solutions to improve the harvesting efficiency [2-6]. In particular, with the technique named *synchronized switch harvesting on inductor* (SSHI), the harvesting capability can increase 450% at most, compared to the PEH with standard interface circuit [4]. Most work on SSHI emphasized its outstanding capability on har-

---

[*] Corresponding author: Tel: (852) 2609 8341; Fax: (852) 2603 6002; E-mail: whliao@cuhk.edu.hk

vesting energy; yet, the energy flow within this treatment was not discussed in depth. This may be due to the limitation of current criterion for evaluating different energy harvesting devices, which usually puts more emphasis on the absolute amount of harvested energy [7]. This paper is aimed to show the energy flow within PEH with SSHI interface circuit. It will be shown that the functions of energy harvesting and energy dissipation are coexistent in the conditioning circuit. In addition, since both energy harvesting and dissipation bring out the effect of structural damping [8, 9], the total damping effect of SSHI will also be investigated.

2. ANALYSIS ON ENERGY FLOW IN SSHI

Until now, most of the researches on energy harvesting focused on how to amend their designs, in order to harvest more energy from vibration sources. The energy flow within the PEH devices was not investigated in detail. Yet, this fundamental understanding is crucial, since it can not only help us clarify the characteristics within these treatments, but also provide us with guidance for the future development on PEH devices.

2-1. Energy flow in piezoelectric devices

In our previous studies [9], the possible energy flows within a piezoelectric device were summarized. The intrinsic relations among energy harvesting, energy dissipation and structural damping were explained. Given a typical piezoelectric device, e.g. a piezoelectric cantilever with shunt circuit, its schematic representation is shown in Figure 1(a). Under harmonic excitation, the possible energy flow is shown in Figure 1(b).
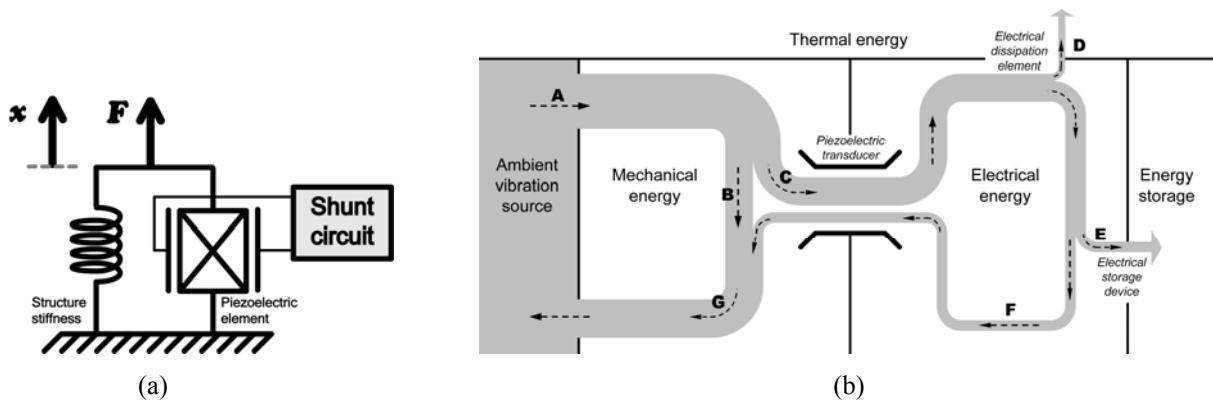

Figure 1. Schematic representation and energy flow chart of a typical piezoelectric device.
(a) Schematic representation. (b) Energy flow chart.

The energy flow chart indicates the directions of energy flow in every vibration cycle. During a cycle, with the electromechanical coupling characteristic of the piezoelectric transducer, some of the input energy (path A) is converted into electrical (path C) and the other returns to the source (path B). Without the shunt circuit, the electrical energy is temporarily stored in the piezoelectric capacitance and then all returns; however, with different shunt circuits connected, this electrical energy may have different destinations. Generally, there are three possible ways: 1) being converted into thermal energy (path D), i.e. dissipated; 2) being stored as energy storage (path E), i.e. harvested; or 3) returning to the source (path F). One or more of these three paths may exist in a certain application. For example, in the application of standard energy harvesting (SEH), the paths of E and F exist but no path D; in resistive shunt damping (RSD), the paths of D and F exist but no path E. In addition, the

total energy return (path G) is combined with both mechanical (path B) and electrical (path F) parts. This energy keeps cycling during every vibration cycle, therefore, it is the energy associated with vibration.

Three terms were defined in [9], in order to provide evaluation and comparison on performances among the three functions of energy harvesting, energy dissipation and structural damping in piezoelectric devices. *Harvesting factor* is defined to evaluate the harvesting capability as

$$\eta_h = \frac{E_h}{2\pi E_{max}} \tag{1}$$

where E_h denotes the harvested energy in one cycle (path E), E_{max} is the energy associated with vibration (path G), multiplying by 2π to obtain the vibratory energy in one cycle. *Dissipation factor* is defined to evaluate the dissipation capability as

$$\eta_d = \frac{E_d}{2\pi E_{max}} \tag{2}$$

where E_d is the dissipated energy in one cycle (path D). With (1) and (2), the *loss factor* is defined as

$$\eta_\Sigma = \frac{\Delta E}{2\pi E_{max}} = \eta_h + \eta_d \tag{3}$$

where ΔE is the summation of E_h and E_d, which represents the total removed energy from the vibrating structure in one cycle. The loss factor is related to the capability on vibration damping, which is the combined effect of both energy harvesting and dissipation.

2-2. Energy flow in SSHI

For the purpose of enhancing the energy conversion efficiency in energy harvesting, Guyomar et al. introduced the SSHI treatment [3-6]. This technique was further specified as "parallel-SSHI" by Lefeuvre et al. [5]. When this treatment circuit is connected to the piezoelectric device, whose model was shown in Figure 1(a), as the shunt circuit, the equivalent circuit of the whole device is shown in Figure 2. Compared to the SEH, the difference lies in the addition of a shunt path, which composes of an active switch *sw* and a small inductor *L* with parasitic resistance *r*.
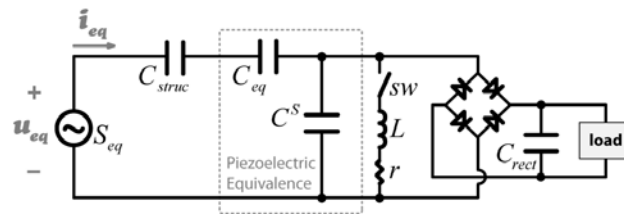

Figure 2. Equivalent circuit for energy harvesting with SSHI technique.

In this equivalent circuit, u_{eq} and i_{eq} are equivalent voltage and current associated with mechanical force F and velocity $\dot{x}$. Their relationships are given by

$$u_{eq} = F/\alpha_e, \qquad i_{eq} = \dot{x}\alpha_e \tag{4}$$

where α_e is the piezoelectric force-voltage coupling factor. It is related to the device piezoelectric coupling coefficient k_d^2 [4] with the relation as follows

$$k_d^2 = \frac{\alpha_e^2}{\left(K_{struc} + K^E\right)C^S + \alpha_e^2} \tag{5}$$

K_{struc} is the structure stiffness; K^E and C^S are short circuit stiffness and clamped capacitance of the piezoelectric element, respectively. C_{struc} and C_{eq} in Figure 2 are related to K_{struc} and K^E with the following relations

$$C_{struc} = \alpha_e^2 / K_{struc}, \quad C_{eq} = \alpha_e^2 / K^E \tag{6}$$

Applying appropriate control to the switch *sw* according to the displacement condition, this treatment can enhance the energy harvesting capability by several hundred percents. The switch is off in most of a cycle; it takes action at the time when the current i_{eq} equals to zero. Also at this instant, the charges stored in the three capacitances are at their extreme values, corresponding to the maximum displacement of the mechanical structure. During the operation, the switch is first turned on to create a "shortcut" for the charge stored in C^S, and then turned off to disconnect the shortcut again when the voltage across C^S alters to another extreme value. Since the electrical cycle, which is decided by the time constant LC^S, is much shorter than the mechanical cycle, the electrical response time can be neglected. Therefore, the voltage waveform can be regarded as changing from V_1 to V_2 steeply at the instant when the current equals to zero. The voltage inversion factor is designated as

$$\gamma = V_2 / V_1 \tag{7}$$

It is related to the Q factor of the switching shunt with the relation given as follows

$$\gamma = -\exp\left(\tfrac{\pi}{2Q}\right) \tag{8}$$

As the electrical part of the device is composed of C^S in parallel with the shunt circuit, Figure 3 shows the typical waveforms of the voltage across it, the current flowing into it, and its power input (product of voltage and current).
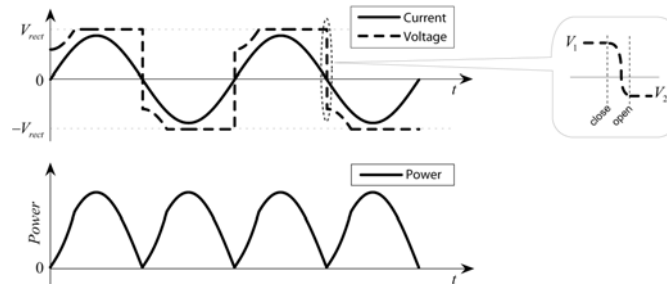

Figure 3. Typical voltage, current and power waveforms in energy harvesting with SSHI technique.

The energy flow in SSHI is different from those in SEH and RSD. In the SSHI treatment, some of the electrical energy is harvested and preserved in the storage device, e.g. C_{rect} in Figure 2; while some of it is dissipated in r during the switch action interval and also in the bridge rectifier throughout every cycle. The first energy dissipation corresponds to the voltage change from V_1 to V_2 across C^S; the second is due to the voltage drop across the rectifier. Moreover, from the power waveform shown in Figure 3, the power input to the electrical part is positive throughout every cycle.

That means no electrical energy returns to the source; all energy converted from mechanical to electrical is either harvested or dissipated. Therefore, the vibratory energy is only composed of mechanical energy. The energy flow chart for SSHI is shown in Figure 4. The electromechanical transduction in this figure is a one way process, which is different from the one in Figure 1(b).
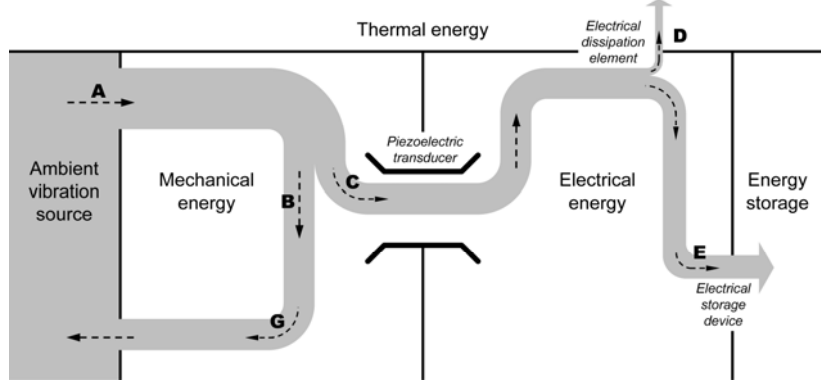

Figure 4. Energy flow chart of PEH devices with SSHI technique.

To quantify the characteristics of energy harvesting, energy dissipation and the effect on vibration damping, the charge-voltage diagram is employed to illustrate the energy conversion cycle. Since the mechanical part of the device, which is represented by C_{struc} and C_{eq} in the equivalent circuit, is in series with the electrical part of the device, the charge flowing through both parts is the same. Given $k_d^2 = 0.3$, $\gamma = -0.2$ ($Q \approx 1.0$) and $\tilde{V}_{rect} = 0.8$, the charge-voltage diagrams of the mechanical and electrical parts are shown in Figure 5(a) and (b), respectively.
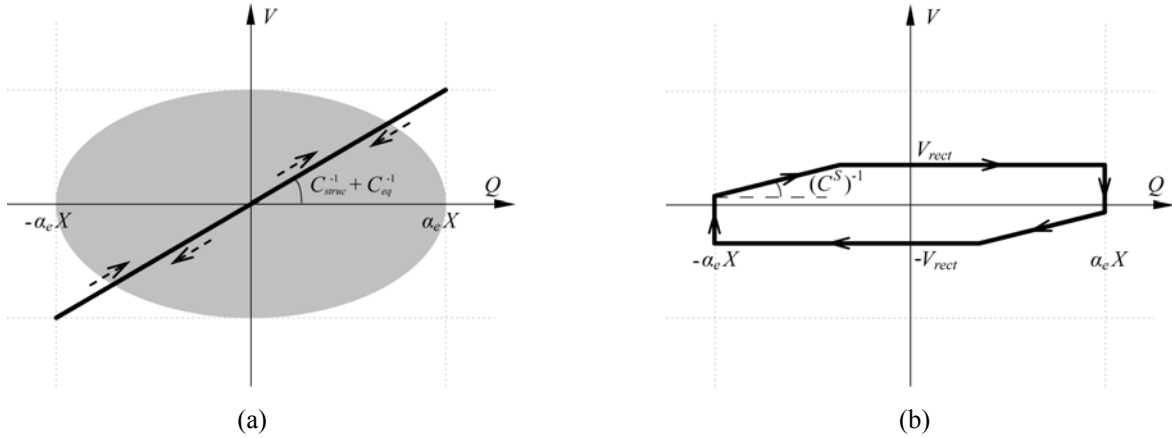

(a)   (b)

Figure 5. Charge-voltage diagrams of the mechanical and electrical parts. (a) Mechanical part. (b) Electrical part.

In Figure 5, X is the maximum displacement of the structure; therefore, $\alpha_e X$ denotes the maximum equivalent input charge. V_{rect} is the rectified voltage. It is the summation of two voltages of V_{store} and V_F, where V_{store} is the voltage across C_{rect} [1] and V_F is the forward voltage drop of the bridge rectifier.

In the charge-voltage diagram of the mechanical part, there is no hysteresis loop. The vibratory energy, i.e. E_{max}, can be estimated as the potential energy under maximum displacement $\alpha_e X$

$$E_{max} = aC^S V_{OC}^2 / 2 \tag{9}$$

---

[1] Since the DC filter capacitor C_{rect} is designed to be much larger than C^S, so V_C is usually regarded constant in every vibration cycle [2-6, 8, 9].

where a stands for the ratio of $(1 - k_d^2)/k_d^2$ and $V_{OC} = \alpha_e X / C^S$, is the open circuit voltage across the piezoelectric element when no shunt circuit is connected. Multiplying 2π to E_{max} yields the energy association with vibration in one cycle, which corresponds to the area of the gray ellipse patch in Figure 5(a).

In the charge-voltage diagram of the electrical part, the area enclosed by the hysteresis loop represents the energy extracted from the source. Both functions of energy harvesting and energy dissipation contribute to the energy extraction. The amount of energy harvested in one cycle is

$$E_h = 2C^S \left(V_{rect} - V_F\right)\left[2V_{OC} - V_{rect}\left(1+\gamma\right)\right] \tag{10}$$

To ensure the harvested energy to be greater than or equal to zero, the range of V_{rect} should be

$$V_F \leq V_{rect} \leq 2V_{OC}/\left(1+\gamma\right) \tag{11}$$

The amount of energy dissipated in one cycle is

$$E_d = C^S V_{rect}^2 \left(1-\gamma^2\right) + 2C^S V_F \left[2V_{OC} - V_{rect}\left(1+\gamma\right)\right] \tag{12}$$

The first item in (12) represents the energy dissipation in r during the switch action interval; the second item results from the voltage drop across the bridge rectifier. Combining the charge-voltage diagrams of the mechanical part and electrical part, and referring to (9)-(11), the charge-voltage diagram of the whole equivalent circuit is shown in Figure 6, with different patterns to indicate different energy flows.
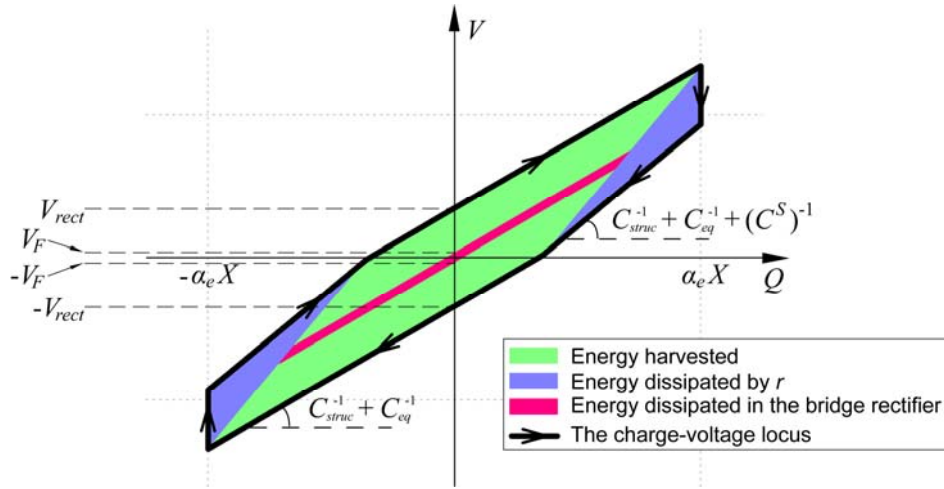

Figure 6. Charge-voltage diagram of the equivalent circuit.

Substituting (9)-(11) for E_d, E_h, E_{max} into (1)-(3), the harvesting factor, dissipation factor and loss factor of this device can be obtained as

$$\eta_h = \frac{2\left(\tilde{V}_{rect} - \tilde{V}_F\right)\left[2 - \tilde{V}_{rect}\left(1+\gamma\right)\right]}{a\pi} \tag{13}$$

$$\eta_d = \frac{\tilde{V}_{rect}^2 \left(1-\gamma^2\right) + 2\tilde{V}_F \left[2 - \tilde{V}_{rect}\left(1+\gamma\right)\right]}{a\pi} \tag{14}$$

$$\eta_\Sigma = \frac{4\widetilde{V}_{rect} - \widetilde{V}_{rect}^2 (1+\gamma)^2}{a\pi} \tag{15}$$

where $\widetilde{V}_{rect}$ and $\widetilde{V}_F$ are respectively the non-dimensional rectified voltage and diode voltage drop, which are defined as

$$\widetilde{V}_{rect} = V_{rect}/V_{OC}, \qquad \widetilde{V}_F = V_F/V_{OC} \tag{16}$$

when k_d^2 and γ are fixed, η_d and η_Σ monotonously increase with $\widetilde{V}_{rect}$, yet η_h is non-monotonic function. The maximum value of η_h can be obtained

$$\eta_{h,max} = \frac{1}{a\pi}\left[\frac{2}{1+\gamma} - 2\widetilde{V}_F + \frac{(1+\gamma)\widetilde{V}_F^2}{2}\right] \tag{17}$$

at an optimum non-dimensional rectified voltage

$$\widetilde{V}_{rect,opt} = \frac{1}{1+\gamma} + \frac{\widetilde{V}_F}{2} \tag{18}$$

When the open circuit voltage V_{OC} is much larger than the forward voltage drop of the bridge rectifier, i.e. V_F, the second item in $\widetilde{V}_{rect,opt}$ can be neglected. Under this condition, referring to (11), the optimum V_{rect} for energy harvesting is half of the upper limit of V_{rect}.

3. EXPERIMENTS

Experiments are performed, in order to verify the theoretical analysis on energy flow in PEH with SSHI interface circuit. With the same experimental setup, but based on different processes, three experiments can be respectively performed to estimate the loss factor, harvesting factor and dissipation factor in the SSHI treatment. Figure 7 shows the mechanical structure and the shunt circuit in the experimental setup.
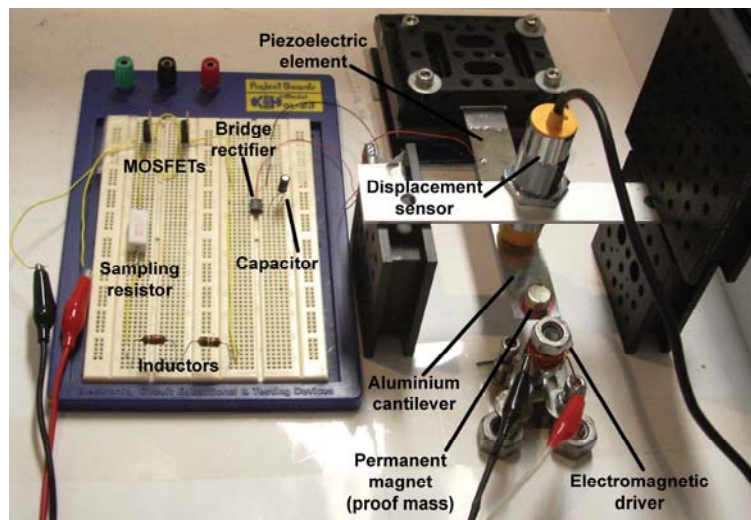

Figure 7. Experimental setup for PEH with SSHI technique.

The main mechanical structure is an aluminium cantilever whose fixed end is fixed on the vibration-free table and the free end is driven by an electromagnetic driver. A piezoceramic patch of 49mm x 24mm x 0.508mm (T120-A4E-602, Piezo System, Inc.) is bonded near the fixed end where the largest strain happens along the cantilever. A permanent magnet is attached at the free end of the cantilever, so as to achieve the coupling with the electromagnetic driver; and it also acts as a proof mass to lower the vibration frequency and increase the displacement of the free end. The displacement of the cantilever is sensed by an inductive displacement sensor (JCW-24SR, CNHF Co.). Applying a 25Hz harmonic excitation, which corresponds to a 1.34V peak-peak value output from the displacement sensor, to this structure, a 16.6V peak-peak value sinusoidal voltage can be observed across the piezoelectric element.

In order to perform SSHI treatment, the displacement sensor output is connected to an A/D channel of the PC based controller board (dSPACE DS1104). The digital processer performs peak detection and generates switch driving signal accordingly to control the switch in SSHI circuit. The shunt circuit is shown on the left hand side of Figure 7. Table 1 gives the models or values of different components in the circuit.

Table 1. Models or values of different components in the shunt SSHI circuit

Component	C^S	sw	L	Bridge Rectifier	C_{rect}	r_{sample}
Value or model	34.76nF	MOSFET (IRF530)	121.8mH	DB104 (V_F= 1.1V)	9.708μF	10.2Ω

The coupling coefficient of the main structure k_d^2 is fixed after fabrication; meanwhile the Q factor of the switching shunt is fixed when all components are connected, i.e. γ is fixed. According to (13)-(15), the three evaluating factors corresponding to structural damping, energy harvesting and energy dissipation are all functions of $\widetilde{V}_{rect}$. The functional relations can be investigated experimentally in the following sections.

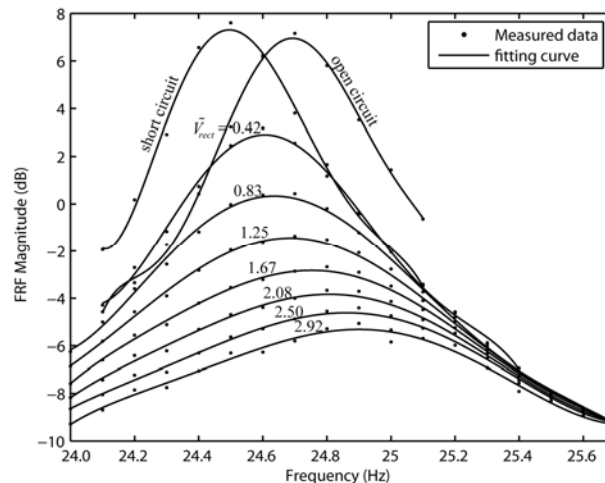## 3-1. Loss factor on structural damping

Figure 8. Frequency response functions under different electrical conditions.

As far as the loss factor is related to the system bandwidth that can be obtained from the frequency response function (FRF) [2], the loss factors under different electrical conditions, i.e. short

---

[2] Strictly, this method for loss factor estimation is valid for linear system. However, since SSHI is a non-linear treatment, this is only an approximation for the loss factor in SSHI treatment.

circuit, open circuit and seven values of $\widetilde{V}_{rect}$ (from 5/12 to 35/12 with a step of 5/12), can be estimated with this method. For each condition, the peak-peak values of the displacement sensor outputs at 18 frequencies (24.0 ~ 25.7Hz with a step of 0.1Hz) are recorded. To obtain the displacement peak-peak values under different $\widetilde{V}_{rect}$, V_{rect} should be adjusted according to the changing V_{OC}, which cannot be directly measured when the SSHI treatment is operating. However, since V_{OC} is proportional to X, the maximum displacement of the structure, it can still be indirectly obtained under SSHI treatment. To adjust V_{rect}, the constant voltage output of a power supply (IPS 2303D, ISO-TECH) is connected to the capacitor C_{rect}. Nine FRF curves are obtained by fitting 18 sets of data under each condition. Figure 8 shows the measured data and fitted curves. For each curve, the resonant frequency f_0 and the -3dB bandwidth Δf can be calculated. Therefore, the loss factor under the corresponding condition is $\Delta f / f_0$. Since the loss factors include both inherent damping and the damping contributed by SSHI, subtracting the loss factors under different $\widetilde{V}_{rect}$ to that under short circuit condition yields the net contribution of the SSHI treatment [8].

3-2. Harvesting factor on energy harvesting

The harvesting factor is estimated based on (1). With the record of a complete charging process, E_h can be obtained from the voltage history across C_{rect}, meanwhile, E_{max} can be obtained from the displacement history. This method was once used to estimate the harvesting factor for SEH [9]. The voltage and displacement histories are separated into a number of appropriate intervals. Within an interval, V_{rect} is regarded as the sum of V_F and the mean voltage across C_{rect}. The energy harvested during this interval can be calculated with respect to the voltage increase across C_{rect}.

E_{max} here only includes mechanical vibratory energy, so it is related to the maximum displacement. Since 1.34V peak-peak value output from the displacement sensor corresponds to 16.6V peak-peak value sinusoidal voltage across the open circuit piezoelectric element, the mechanical vibratory energy associated with 1.34V peak-peak value displacement output can be estimated with the device coupling coefficient, which can be calculated with the resonant frequencies under open circuit and short circuit conditions with the following relation

$$k_d^2 = \frac{f_{OC}^2 - f_{SC}^2}{f_{OC}^2} \tag{19}$$

From Figure 8, f_{OC} = 24.69Hz, f_{SC} = 24.50Hz, therefore k_d^2 = 0.0153. This means, in the open circuit, when the voltage across C^S is at maximum, i.e. 8.8V, the ratio between mechanical energy and electrical energy is a, which is defined above as $(1-k_d^2)/k_d^2$. Knowing the E_{max} associated with 1.34V peak-peak value displacement output, the E_{max} associated with other values can be obtained.

3-3. Dissipation factor on energy dissipation

The dissipation factor is estimated based on (2). From the voltage across C^S, the voltage inversion factor γ is obtained to be -0.384. So the Q factor of the switching shunt is about 1.64, the total equivalent series resistance r is 1.14 kΩ. Since a 10 Ω sampling resistor r_{sample} is connected in series to the shunt, recording the root mean square (RMS) voltage across r_{sample} under different V_{rect} with an oscilloscope (TDS 220, Tektronix), the energy consumed by r in one cycle can be estimated. As for the energy dissipated by the bridge rectifier in one cycle, i.e. the second item in (12), it is proportional to E_h under certain V_{rect}; therefore it can be calculated simultaneously with the estimation of E_h. Combining these two dissipations, E_d is readily to be obtained.

3-4. Results

Three experiments are performed in order to show the functional relations with either of η_h, η_d and η_Σ to $\tilde{V}_{rect}$. Besides, since k_d^2 and γ are experimentally obtained as 0.0153 and -0.384, respectively, the three evaluating factors are also readily to be theoretically obtained with (13)-(15). Both results are simultaneously shown in Figure 9. It demonstrates that both experimental results and theoretical analyses agree with each other very well.
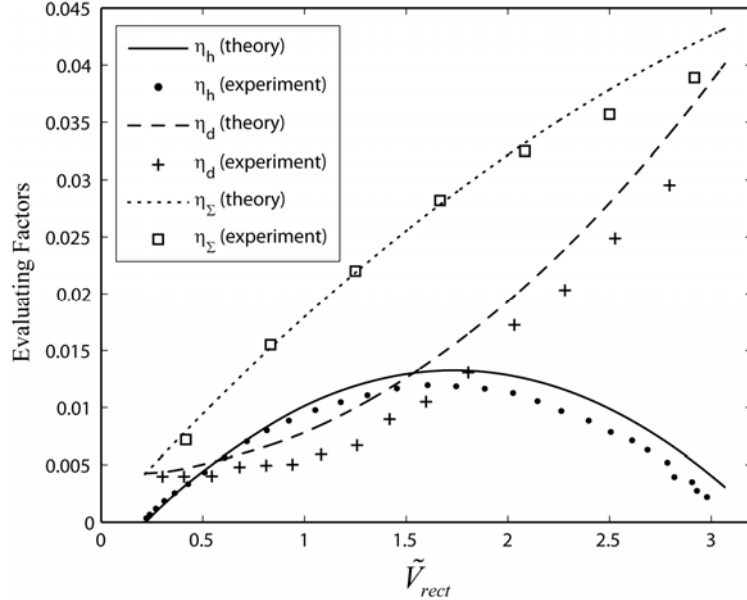

Figure 9. Theoretical and experimental results on three evaluating factors in PHE with SSHI interface.

4. CONCLUSIONS

This paper presented detailed analyses on the energy flow in PEH with SSHI interface. The concept of energy flow was clarified and illustrated with energy flow chart. Previously, absolute harvesting power was usually considered to evaluate different PEH devices. This is an application-oriented evaluation. But looking into the PEH devices, for an overall evaluation, we suggest that three evaluating factors are likewise important, since they are helpful to show the energy flow within different PEH devices. In the PEH with SSHI interface, quantitative analyses verified the coexistent relation between energy harvesting and energy dissipation and also their effect on structural damping. Even it was reported that the SSHI treatment can significantly enhance the harvesting efficiency, it also follows by the increase on energy dissipation. In particular, for larger $\tilde{V}_{rect}$, the dissipation factor can be larger than the harvesting factor, i.e. more energy is dissipated rather than harvested in one cycle. This should be avoided for the purpose of making good recycling of the ambient vibration energy.

Generally speaking, in every PEH device, energy dissipation inevitably exists. Even for SHE devices, the bridge rectifier consumes energy because of its forward voltage drop. The coexistent relation between energy harvesting and dissipation is subtle. The understanding on their relation and their total effect to the vibrating structure is crucial towards future development on PEH devices.

REFERENCES

1. S. R. Anton and H. A. Sodano, "A review of power harvesting using piezoelectric materials (2003-2006)," *Smart Materials and Structures*, vol. 16, no. 3, pp. R1-R21, 2007.
2. G. Ottman, H. Hofmann, A. Bhatt, and G. Lesieutre, "Adaptive piezoelectric energy harvesting circuit for wireless remote power supply," *IEEE Transactions on Power Electronics*, vol. 17, no. 5, pp. 669-676, 2002.
3. D. Guyomar, A. Badel, E. Lefeuvre and C. Richard. "Toward energy harvesting using active materials and conversion improvement by nonlinear processing," *IEEE Transactions on Ultrasonics, Ferroelectrics and Frequency Control*, vol. 52, no. 4, pp. 584-595, 2005.
4. A. Badel, D. Guyomar, E. Lefeuvre and C. Richard, "Efficiency enhancement of a piezoelectric energy harvesting device in pulsed operation by synchronous charge inversion," *Journal of Intelligent Material Systems and Structures*, vol. 16, no. 10, pp. 889-901, 2005.
5. E. Lefeuvre, A. Badel, C. Richard, L. Petit and D. Guyomar, "A comparison between several vibration-powered piezoelectric generators for standalone systems," *Sensors and Actuators A: Physical*, vol. 126, no. 2, pp. 405–416, 2006.
6. Y. C. Shu, I. C. Lien and W. J. Wu, "An improved analysis of the SSHI interface in piezoelectric energy harvesting," *Smart Materials and Structures*, vol. 16: pp. 2253–2264, 2007.
7. S. Beeby, M. Tudor, and N. White, "Energy harvesting vibration sources for microsystems applications," *Measurement Science and Technology*, vol. 17, no. 12, pp. R175–R195, 2006.
8. G. A. Lesieutre, G. K. Ottman and H. F. Hofmann, "Damping as a result of piezoelectric energy harvesting," *Journal of Sound Vibration*, vol. 269, pp. 991–1001, 2004.
9. J. R. Liang and W. H. Liao, "Energy harvesting and dissipation with piezoelectric materials," *Proceedings of the 2008 IEEE International Conference on Information and Automation*, pp. 446-451, 2008.